J. Synchrotron Rad. (1998). **5**, 762–765

Calibration of space-resolving VUV and soft X-ray spectrographs for plasma diagnostics

Masayuki Yoshikawa,[a]* Naohiro Yamaguchi,[b] Tatsuya Aota,[a] Katsunori Ikeda,[a] Yuuji Okamoto,[a] Kiyoshi Yatsu[a] and Teruo Tamano[a]

[a]Plasma Research Center, University of Tsukuba, Tsukuba, Ibaraki 305, Japan, and [b]Toyota Technological Institute, 2-12-1 Hisakata, Tempaku, Nagoya 468, Japan.
E-mail: yosikawa@prc.tsukuba.ac.jp

(*Received 4 August 1997; accepted 10 November 1997*)

Vacuum ultraviolet (VUV) and soft X-ray measurements are important means of diagnosing impurities in magnetically confined plasmas used in fusion research. Recently, space- and time-resolving flat-field VUV (150–1050 Å) and soft X-ray (20–350 Å) spectrographs have been constructed by using aberration-corrected concave gratings with varied-spacing grooves which give a wide simultaneous spectral coverage on a microchannel-plate intensified detector. Calibration experiments have been performed at beamlines 11A and 11C at the Photon Factory of the High Energy Accelerator Research Organization. The relative efficiency of the VUV spectrograph has been measured for *P*-polarization geometry in the spectrograph. In the soft X-ray spectrograph, efficiencies have been obtained for several different points of irradiation on the grating along the groove direction and for two (*S* and *P*) polarization geometries.

Keywords: VUV spectrographs; soft X-ray spectrographs; plasma diagnostics.

1. Introduction

Impurity lines and continuum radiation emitted from high-temperature plasmas are in the wavelength range from vacuum ultraviolet (VUV) to X-ray. These emissions provide us with information on the radiation power losses and the ion density profiles which relate directly to the impurity transport in magnetically confined plasmas. Therefore, VUV and soft X-ray measurements are important means of diagnosing such plasmas used in fusion research. In plasmas produced in the tandem mirror GAMMA 10, the electron temperature is rather low compared with the ion temperature in the central mirror region (Inutake *et al.*, 1993; Tamano, 1995). VUV and soft X-ray spectroscopic measurements provide information about confined core plasmas and are important in tandem mirror research. These measurements require instruments that provide simultaneous spectral, temporal and spatial resolution of the plasma radiation.

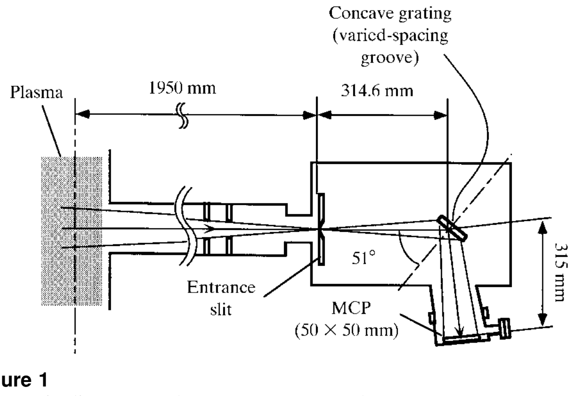

Figure 1
Schematic diagram of the VUV spectrograph.

Recently, we have also constructed space- and time-resolving spectrographs in the VUV and soft X-ray region (Yamaguchi, Kato, Sato, Aota, Mase & Tamano, 1994; Yamaguchi, Kato, Sato, Aota, Mase, Nakashima & Tamano, 1994; Yamaguchi, Aota *et al.*, 1995; Yamaguchi, Sato *et al.*, 1995; Yamaguchi *et al.*, 1997; Yoshikawa *et al.*, 1996).

This article describes the design and calibration experiments of the VUV and soft X-ray spectrograph with aberration-corrected concave gratings for simultaneous observation of spatial and spectral distributions of plasmas confined in large magnetic fusion devices.

2. Spectrograph description

2.1. *VUV spectrograph*

Fig. 1 shows a schematic diagram of the VUV spectrograph on GAMMA 10. The pressure inside the spectrograph is kept below 1×10^{-7} torr by using two turbomolecular pumps. The VUV spectrograph can provide spatial and spectral distributions of plasma radiation in the wavelength range 150–1050 Å. It consists of an entrance slit of limited height (100 µm × 2 mm), an aberration-corrected concave grating with varied-spacing grooves (Hitachi P/N001-0464), which gives a flat-field spectral output plane, and an image-intensified two-dimensional detector system. The specifications of the grating are a radius of curvature of 500 mm, nominal groove density 1200 grooves mm^{-1}, braze angle 3.08°, ruled area 48 × 48 mm, incident angle 51°, and effective braze wavelength 600 Å. One can observe the upper half of the plasma with a field of view of about 25 cm diameter. The detector system consists of an MCP intensified image detector assembly (Hamamatsu F2814-23P, 50 × 50 mm) and two types of image-recording camera: one is an instant photographic camera and the other is a high-speed solid-state camera (Reticon MC9256) with a fast scanning controller. The frame rate with full image size, 256 × 256 pixels, can be changed from 4 to 106 frames s^{-1}. When the number of lines whose data are to be read is reduced and the remaining lines are skipped, one can increase the frame rate up to 1000 frames s^{-1}. While one can obtain a snapshot of a space-resolving spectrum with 1 ms temporal resolution by gating the

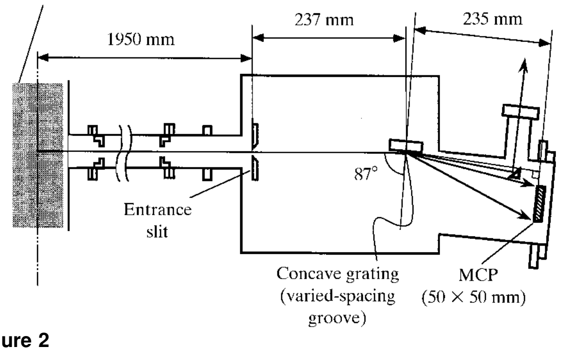

Figure 2
Schematic diagram of the soft X-ray spectrograph.

MCP response in each plasma shot by using an instant camera, sequential space-resolving spectra can be obtained in a single plasma shot with a temporal resolution by using the solid-state camera.

2.2. *Soft X-ray spectrograph*

A schematic diagram of the optical system of the soft X-ray spectrograph is shown in Fig. 2. This is a grazing-incidence spectrograph with an incident angle of 87° and effective braze wavelength of 100 Å. The grating, designed to cover the 20–350 Å wavelength range with flat focal field, has a radius of curvature of 5649 mm, a nominal groove density of 1200 grooves mm^{-1}, a braze angle of 3.2° and a ruled area of 50 × 30 mm (Hitachi P/N 001–0266). The entrance slit is placed 1.95 m away from the centre of the plasma and has an opening 100 μm wide by 2 mm high. This spectrograph is also placed on GAMMA 10 so as to observe the upper half of a plasma about 20 cm in radial direction. Two rectangular opening baffles are positioned at both ends of the coupling vacuum duct to prevent stray light from entering the spectrograph. The detection system is the same as that of the VUV spectrograph.

3. Calibration of the spectrograph

3.1. *Calibration of the VUV spectrograph*

A calibration experiment has been performed using synchrotron radiation at the Photon Factory in the High Energy Accelerator Research Organization (BL-11C) (Yamaguchi *et al.*, 1997). The incident photon intensity was monitored just behind the entrance slit by using an XUV silicon photodiode (IRD AXUV 100) and the output spectral image was recorded on an instant film (Fuji FP-3000B). The relative efficiency of the XUV silicon photodiode was measured at the Photon Factory, but not the absolute efficiency. Measurements were repeated for incident wavelengths from 300 to 1150 Å at intervals of 50 Å at the central point of the grating along the groove direction. Recorded images were analysed by using an image scanner (Epson GT-6000) and a personal computer. Fig. 3 shows the relative efficiency of the spectrograph for the first-order diffracted light as a function of wavelength including the film response of the instant film (Yamaguchi, Kato, Sato, Aota, Mase & Tamano, 1994). The influence of the higher-order diffracted light for this spectrograph can be neglected. These experiments were carried out under the *P* polarization of the spectrograph. The position of a peak (at 600 Å) corresponds to the braze wavelength of the grating used in this spectrograph.

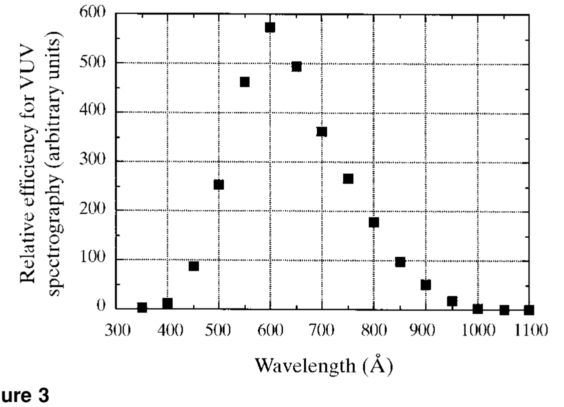

Figure 3
Relative efficiency for the first-order diffracted light for the VUV spectrograph against wavelength.

3.2. *Calibration of the soft X-ray spectrograph*

Calibration experiments have been performed at beamline 11A at the Photon Factory (Yamaguchi, Aota *et al.*, 1995). They have been carried out by monitoring the incident photon intensity just behind the entrance slit by using the XUV silicon photodiode and then measuring the output image. Measurements were repeated for incident wavelengths from 50 to 140 Å under two (*S* and *P*) polarization geometries in the spectrograph. The experimental procedure is the same as that of the VUV spectrograph experiments. We measured three different points (z = 0, +10, +20 mm) on the upper half of the grating for *P* polarization and five points (z = −10, −6, 0, +8, +14 mm) on the whole grating along the groove direction for *S* polarization. Fig. 4 shows the relative efficiency of the spectrograph for the first-order diffracted light as a function of wavelength including the film response of the instant film. The differences of the efficiencies against their irradiation positions are larger in the shorter-wavelength range. In this spectrograph it should be noted that the higher-order diffracted light is not weak enough to be neglected, since we have observed the higher-order diffracted light in these experiments.

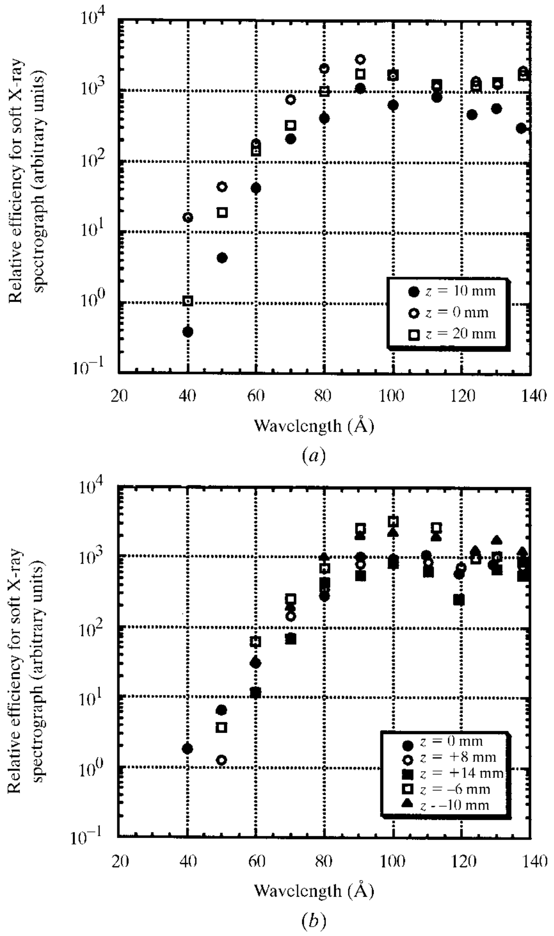

Figure 4
Relative efficiency for the first-order diffracted light for the soft X-ray spectrograph against wavelength, (*a*) for *P* polarization and (*b*) for *S* polarization.

4. VUV/soft X-ray spectroscopy on GAMMA 10

The VUV and soft X-ray spectrographs have been placed in the central cell region of GAMMA 10. In GAMMA 10, plasma confinement is achieved by not only a magnetic mirror configuration but also positive high potentials at the end regions. The plug potential is produced by means of electron cyclotron resonance heating (ECRH) at the plug/barrier region. The main plasma confined in GAMMA 10 is produced and heated by ion cyclotron range of frequency (ICRF) power deposition. Space- and time-resolved spectra have been obtained successfully in the GAMMA 10 experiments. Fig. 5 shows the VUV spectral images taken using the high-speed camera with 30 ms time resolution. Almost all lines are observed within a region of about 10 cm radius, because the plasma density profile has about 10 cm radius in full width at half-maxima, and they are identified as spectral lines of C or O ions. Soft X-ray spectral images were taken using the instant camera with 1 ms time resolution. There are few spectral lines in the shorter-wavelength region. There is very little influence of the higher-order diffracted light on the measured spectrum in our experiments.

5. Analysing method of space-resolved spectral images

We analysed spatially resolved VUV spectrophotographs using the following procedure (Yoshikawa *et al.*, 1996). First, a brightness profile for a given wavelength interval was obtained from a space-resolved spectral image after correction of the film response and the relative efficiency of the spectrograph. This procedure was carried out along the full wavelength range in the spectrophotograph. Next, the brightness profile of each wavelength was transformed to an Abel inverted profile. Then, each Abel inverted profile was reconstructed in a two-dimensional image as shown in Fig. 6. Fig. 6 shows the reduced spectral distribution of the recorded VUV spectrum (Fig. 5) after correction with the relative efficiency of the spectrograph. The difference of the efficiency for the VUV spectrograph against the radiating positions is neglected because the radial profile of radiation components obtained from the time-of-flight neutral particle analyser was the same as that from the VUV spectrograph (Yamaguchi *et al.*, 1994). Thus, one can investigate the emissivity profile of each spectral source in a visual way from a spatially resolved VUV spectrophotograph.

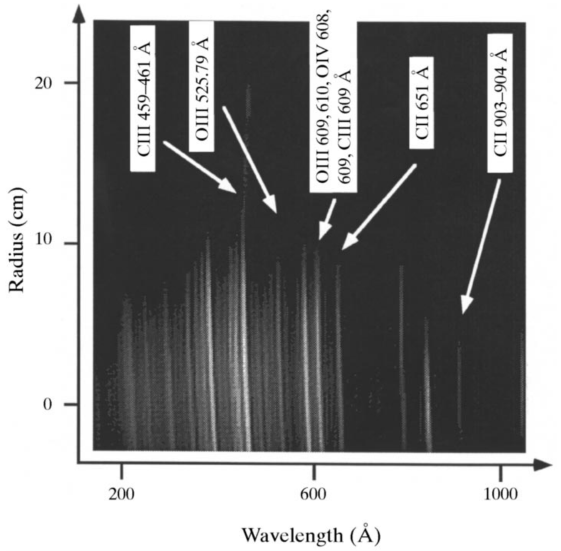

Figure 5
VUV spectral image taken at the central cell in GAMMA 10.

Analysis of the soft X-ray spectrographic data would be more complicated than that of VUV data because the higher-order diffracted light might not be neglected. However, we can obtain the relative efficiency in the wavelength range 50–150 Å for the first-order diffracted light.

6. Conclusions

New spatial imaging VUV and soft X-ray spectrographs have been constructed and their relative efficiency for the first-order diffracted light against wavelength has been calibrated. Space- and time-resolved spectra have been obtained successfully in GAMMA 10. Moreover, we established a method of obtaining the emissivity profile images from the spectral images. However, the calibration experiments of the soft X-ray region were unable to cover the whole wavelength range of the soft X-ray spectrograph. Light from the beamline was also unable to irradiate the whole grating area. We are now considering another experiment to obtain the efficiency of the whole wavelength range of the soft X-ray spectrograph and the efficiency of the irradiation position of the grating at the same time.

The authors would like to thank members of the GAMMA 10 group of the University of Tsukuba for their collaboration. Part of this work was supported by a Grant-in-Aid for Scientific Research (Contract No. 08780480) from the Ministry of Education, Science and Culture, Japan, and by a University of Tsukuba Project Research. Part of the work has been performed under the approval of the Photon Factory Advisory Committee (Proposal No. 93-G323, No. 96-G140).

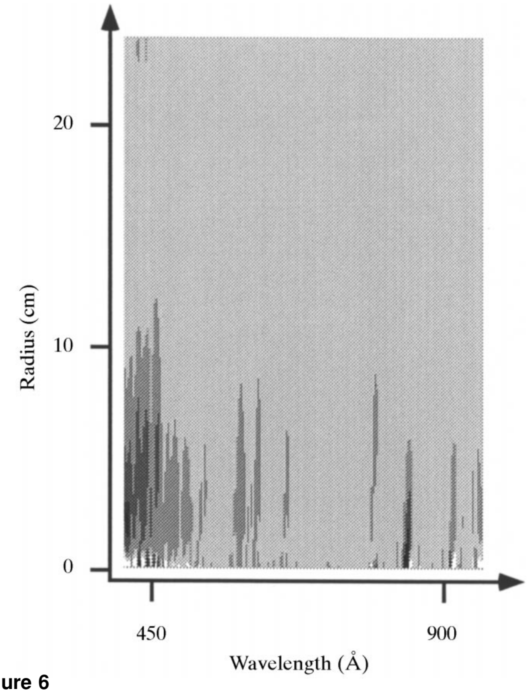

Figure 6
Spectral emissivity in the VUV region.

References

Inutake, M., Tamano, T., Cho, T., Hirata, M., Hojo, H., Ichimura, M., Ishii, K., Itakura, A., Katanuma, I., Kiwamoto, Y., Mase, A., Miyoshi, S., Nagayama, Y., Nakashima, Y., Saito, T., Tatematsu, Y., Yamaguchi, N., Yatsu, K., Yasaka, Y., Sakai, O., Shima, M., Yoshida, H. & Itatani, R. (1993). *Nucl. Fusion Suppl.* **2**, 651–658.

Tamano, T. (1995). *Phys. Plasmas*, **2**, 2321–2327.

Yamaguchi, N., Aota, T., Ikeda, K., Cho, T., Aoki, S., Mase, A., Maezawa, H. & Tanaka, K. (1995). Photon Factory Activity Report 1994, p. 238. National Laboratory for High Energy Physics, Tsukuba, Ibaraki 305, Japan.

Yamaguchi, N., Aota, T., Ikeda, K., Yoshikawa, M., Okamoto, Y. & Ishijima, T. (1997). Photon Factory Activity Report 1993, p. 224. National Laboratory for High Energy Physics, Tsukuba, Ibaraki 305, Japan.

Yamaguchi, N., Kato, J., Sato, Y., Aota, T., Mase, A., Nakashima, Y. & Tamano, T. (1994). *International Conference on Open Plasma Confinement Systems for Fusion*, edited by A. A. Kabantsev, pp. 221–229. London: World Scientific.

Yamaguchi, N., Kato, J., Sato, Y., Aota, T., Mase, A. & Tamano, T. (1994). *Rev. Sci. Instrum.* **65**, 3408–3414.

Yamaguchi, N., Sato, Y., Kato, J., Aota, T., Ikeda, K., Mase, A. & Tamano, T. (1995). *J. Plasma Fusion Res.* **71**, 867–875.

Yoshikawa, M., Aota, T., Ikeda, K., Ishijima, T., Okamoto, Y., Yamaguchi, N., Mase, A. & Tamano, T. (1996). *Proceedings of the 1996 International Conference on Plasma Physics*, edited by H. Sugai & T. Hayashi, pp. 1470–1473. Nagoya: Jpn. Soc. Plasma Sci. Nucl. Fusion Res.